



Characteristics of sensory innervation in synovium of rats within different knee osteoarthritis models and the correlation between synovial fibrosis and hyperalgesia



Li Zhang^{a,b,c}, Mingchao Li^{a,c}, Xiaochen Li^{a,b,c}, Taiyang Liao^{a,b,c}, Zhenyuan Ma^{a,b,c}, Li Zhang^{a,b}, Runlin Xing^{a,b}, Peimin Wang^{a,b}, Jun Mao^{a,b,*}

^aThe Affiliated Hospital of Nanjing University of Chinese Medicine, Department of Orthopedics, Nanjing 210029, China

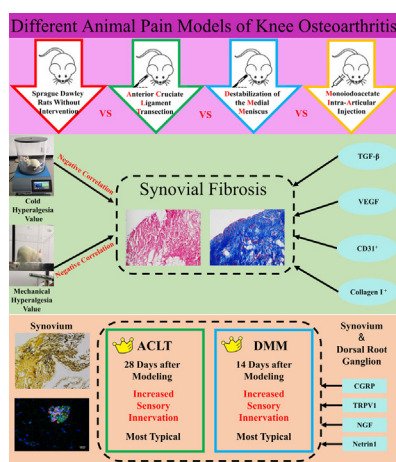
^bJiangsu Province Hospital of Chinese Medicine, Nanjing, Jiangsu 210029, China

^cKey Laboratory for Metabolic Diseases in Chinese Medicine, First College of Clinical Medicine, Nanjing University of Chinese Medicine, Nanjing 210023, China

HIGHLIGHTS

- Synovial fibrosis was positively correlated with pain sensitivity in KOA rats.
- Synovial fibrosis was most prominent in DMM group 14 days after modeling.
- ACLT replaced DMM to be the most typical at 28 days after modeling.
- Increased synovial sensory innervation followed the same trend as fibrosis.
- ACLT is more applicable for KOA pain research.

GRAPHICAL ABSTRACT



ARTICLE INFO

Article history:

Received 12 April 2021

Revised 7 June 2021

Accepted 8 June 2021

Available online 15 June 2021

Keywords:

Knee osteoarthritis
Animal models
Pain
Synovial fibrosis
Sensory innervation

ABSTRACT

Introduction: Knee osteoarthritis (KOA) showed synovial fibrosis and hyperalgesia, although the correlation between the two is unclear. Besides, the specific changes of sensory innervation in animal models are still controversial, which makes it difficult to choose the modeling methods for KOA pain research.

Objectives: Study the characteristics of sensory innervation within three commonly used KOA rat models and the correlation between synovial fibrosis and hyperalgesia.

Methods: KOA models were induced by destabilization of medial meniscus (DMM), anterior cruciate ligament transection (ACLT), and monoiodoacetate (MIA), respectively. Mechanical, cold and thermal withdrawal threshold (MWT, CWT and TWT) were measured. The harvested tissues were used for pathological sections, immunofluorescence and quantitative analysis.

Results: KOA synovium showed more type I collagen deposition, increased expression of CD31, VEGF and TGF-β. These changes were most pronounced in surgical models, with DMM presenting the most

Abbreviations: KOA, knee osteoarthritis; CGRP, calcitonin gene-related peptide; TRPV1, transient receptor potential vanilloid type 1; NGF, nerve growth factor; DMM, destabilization of the medial meniscus; MIA, monoiodoacetate; ACLT, anterior cruciate ligament transection; ECM, extracellular matrix; TGF-β, transforming growth factor-β; VEGF, vascular endothelial growth factor; MWT, mechanical withdrawal threshold; TWT, thermal withdrawal threshold; CWT, cold withdrawal threshold.

Peer review under responsibility of Cairo University.

* Corresponding author at: The Affiliated Hospital of Nanjing University of Chinese Medicine, Department of Orthopedics, Nanjing 210029, China.

E-mail address: junmao1978@hotmail.com (J. Mao).

<https://doi.org/10.1016/j.jare.2021.06.007>

2090-1232/© 2021 The Authors. Published by Elsevier B.V. on behalf of Cairo University.

This is an open access article under the CC BY-NC-ND license (<http://creativecommons.org/licenses/by-nc-nd/4.0/>).

prominent at Day 14 and ACLT at Day 28. Day 14, changes in mechanical hyperalgesia and cold hyperalgesia were most typical in DMM model and statistically different from MIA. There was a negative correlation between the percentage of type I collagen and MWT value ($r = -0.88$), as well as CWT value ($r = -0.95$). DMM synovium showed more axonal staining, upregulated CGRP, TRPV1, NGF and Netrin1 compared with MIA. Above changes were also observed at Day 28, but ACLT replaced DMM as the most typical. In DRG, only the levels of CGRP and NGF were different among KOA models at Day 14, and the highest in DMM, which was statistically different compared with MIA.

Conclusions: This study described the details of sensory innervation in different KOA model of rats, and the degree of synovial fibrosis was positively correlated with the pain sensitivity of KOA model rats. Additionally, surgical modeling especially ACLT method is more recommended for KOA pain research.

© 2021 The Authors. Published by Elsevier B.V. on behalf of Cairo University. This is an open access article under the CC BY-NC-ND license (<http://creativecommons.org/licenses/by-nc-nd/4.0/>).

Introduction

Knee osteoarthritis (KOA) is the most prominent form of synovial joint disease, which includes joint degeneration, intermittent inflammation, and peripheral neuropathy [1]. Joint pain is the first and foremost clinical symptom of KOA patients and a medical problem urgently to be solved. As disease advances, ongoing inflammatory stimulation and progressive damage to local tissues, such as synovial inflammation and cartilage degradation, may lead to pain sensitivity, the abnormal responsiveness from changes in nociceptive processing in the peripheral or central nervous system [2,3]. In consequence, neither the degree of subchondral bone degeneration shown on X-Ray, nor the volumetric change of synovium evaluated under magnetic resonance imaging is consistent with KOA pain, which also makes it more difficult to study the pain from KOA [2,3]. Besides, as the main pathological changes of KOA synovium, synovitis has always been considered to cause pain perception directly, but whether synovial fibrosis, one outcome of synovitis, could lead to pain remains controversial [4,5]. Therefore, further efforts are still needed in discovering the pathological mechanisms of KOA, especially those related to pain.

Sensory innervation consists of nerve fibers and receptors, which are directly involved in the pain delivery. In KOA, small-diameter dorsal root ganglion (DRG) neurons and associated A δ -fiber, C-fiber afferents located in Lumbar 3-5 are critical for detecting noxious stimuli and initiating pain sensation. DRG respond to stimuli and transmit stimulus signals to the spinal cord, emerging up-regulations of the immediate early gene *c-fos* [6]. And those perivascular, unmyelinated nerve fibers containing calcitonin gene-related peptide (CGRP) are also implicated in mediating sustained burning pain described by KOA patients [7]. A similar situation occurs in transient receptor potential vanilloid type 1 (TRPV1), a ligand-gated calcium ion (Ca²⁺) channel expressed in sensory neurons and nerve endings in synovium, has been confirmed to mediate peripheral hyperalgesia and considered to be nociceptor of KOA [8]. Besides, nerve growth factor (NGF) is widely recognized as a mediator of chronic pain. Evidence for the contribution of NGF to KOA pain includes increased NGF in synovial fluid, at the synovium and cartilage [9].

Animal models are perfect candidates for laboratory studies of KOA pain [10–12]. Surgical destabilization of the knee is often used to mimic the mechanical instability that occurs in human knees of KOA. Among them, anterior cruciate ligament transection (ACLT) and destabilization of the medial meniscus (DMM) are the most commonly used surgical techniques [13]. ACLT changes were identical to human KOA histological findings, such as cartilage damage, subchondral sclerosis, and osteophyte formation, while the changes caused by DMM are more modest. Intra-articular injection of monosodium iodoacetate (MIA) or collagenase creates other models for the study of acute cartilage degradation and joint pain. However, since MIA is a metabolic poison, chondrocyte cell death in this model

is extensive, unlike in human KOA [10–14]. Recently, using the KOA model mice induced by DMM, Obeidat et al reported an increase of fibers and nociceptors in the deeper layers of the medial synovium [15]. This increased nociceptive innervation could also be observed in subchondral bone of the DMM mice, and be blamed for the Netrin1, a secreted axon guidance molecule that can trigger attraction or repulsion by binding to different receptors, induced sensory nerve axonal growth [16]. In contrast, others reported decrease in sensory innervation in the synovium, particularly peptidergic fibers, with collagenase-induced or MIA models [17–19]. It is difficult to determine whether this discrepancy is due to different modeling approaches, but such results truly make it difficult to choose experimental models. According to Miller, of the animal models used for KOA pain research, MIA model accounted for 54%, surgery model, mainly DMM and ACLT, for 28%, and collagenase-induced model for 3%, since 2008 [13]. Meanwhile, a parallel comparison of sensory innervation in synovium of rats within different KOA models, to our knowledge, has not yet been reported.

In addition, all experimental models of KOA-like joint damage are accompanied by synovial fibrosis, an imbalance caused by the extracellular matrix (ECM) disturbance and vascular hyperplasia. Transforming growth factor- β (TGF- β) and vascular endothelial growth factor (VEGF) play the central roles in the fibrotic cascade [20,21]. Previous studies have proven synovial fibrosis in KOA was accompanied with angiogenesis like RA, and highly associated with VEGF [22]. The angiogenesis marker CD31 has also been shown to be highly expressed in synovium from patients with KOA. On the other hand, specific angiogenesis inhibitor PPI-2458 could reduce pain behavior and TGF- β might stimulate NGF production in KOA rats [23,24], suggesting that synovial fibrosis may be one of the reasons leading to pain, although the correlation between them remains poorly understood.

Therefore, in this study, three different kinds of KOA models were constructed to observe the sensory innervation and fibrosis in synovium, aiming to describe distinction of these models in KOA pain research and to study the correlation between synovial fibrosis and pain.

Material and methods

Ethics statement

All experiments involving animals were conducted according to the ethical policies and procedures approved by the Animal Care and Use Committee of the Nanjing University of Chinese Medicine (Approval no. 201905A002).

Animal experimental design

Eighty SD male rats, weight ranging from 240 g to 280 g (provided by Nanjing Qinglongshan Animal Farm), were used. Animals

were housed in a specific pathogen-free, laminar-flow housing apparatus under controlled temperature, humidity and 12 h light/dark regimen, and maintained on standard rodent pellet diet. Rats were randomly numbered and divided into four groups: Normal, ACLT, DMM, MIA. After one week of adaptive feeding, modeling started and that day was recorded as Day 0. Experimental animals were anesthetized with Nembutal and all the modeling procedures were performed by six researchers with orthopedic surgery background on the same day. Briefly, the medial meniscotibial ligament in the DMM model was transected while in the ACLT model the anterior cruciate ligament was destroyed as described previously [14], both knees. MIA model was induced by intra-articular injection of 1 mg monosodium iodoacetate (MIA), dissolved in 50 μ l sterilized physiologic saline, both knees.

Behavioral tests for KOA pain

Behavioral testing was conducted within ten rats from each group on Day14 and Day 28, respectively. The mechanical withdrawal threshold (MWT) was applied for assessing mechanical allodynia by use of a calibrated electronic von Frey filament (BME404, Institute of Biomedical Engineering, Chinese Academy of Medical Sciences) on the plantar surface of hind paws as described previously [25]. Thermal withdrawal threshold (TWT) and cold withdrawal threshold (CWT) were employed to determine the pain response to a radiant heat (50 ± 2 °C) or cold (0 ± 2 °C) with a temperature-adjustable plate system (35150–001, Ugo Basil SLR, Italy). Recorded the values if the rat exhibits rapid reactions, such as clawing, lifting, or licking feet. Each process was repeated thrice with a 10-minute interval.

Histological analysis

Synovial tissues were fixed in 10% neutral formalin after rats executed, embedded in paraffin, and cut into slices, for routine HE staining. Sirius red and Masson staining were carried out according to the instructions of Sirius Red Stain Kit and Masson's Trichrome Stain Kit (Solarbio Life Sciences, Beijing, China), respectively. Sections were mounted and viewed under a Leica DMI3000B microscope (Leica, Germany) or a Nikon Eclipse E100 (Nikon, Japan), with the use of bright field. Semi-quantification of synovial fibrosis was evaluated by calculating the percentage of collagen I positive areas with ImageJ.

Silver staining for nerve fibers

The paraffin sections were dewaxed with xylene and anhydrous ethanol and then invaded into the acidic formaldehyde dye. After washing, sections were immersed into the glycine silver dye. Finally, the water seal slices were stained with the reducing solution and the images were collected with a Nikon Eclipse E100 (Nikon, Japan).

Table 1
Nucleotide sequences of primers used for RT-PCR amplification.

Target gene	Forward primer	Reverse primer
TRPV1	CAGCGAGTTCAAAGACCCAGAGAC	GGAGCAGAGCGATGGTGTCAATC
CGRP	ATCTGGTCCTTCTCACACTGTCC	TCATCCGTCTTCAGCTTGGCAATC
NGF	CCAGCCTCCACCCACCTCTTC	GCTTGCTCTGTGAGTCTCTGTTG
Netrin-1	CCTTCTCACCAGACCTCAACAATC	CTTCTTGCCGAGCCACAGAGTG
TGF- β	TGCGCCTGCAGAGATCAAG	AGACAGCCACTCAGGCGTAT
VEGF	CACGACAGAAGGGGAGCAGAAAG	GGCACACAGGACGGCTTGAAG

Immunohistochemical (IHC)

Briefly, sections were incubated in antigen retrieval buffer to unmask the antigen after a standard deparaffinization and rehydration process. Sections were treated with hydrogen peroxide, then Triton X-100, and blocked with BSA. The primary antibody and species-matched HRP-labelled secondary antibody were added successively. DAB was used as chromogen and hematoxylin was used to counterstain. Images were captured and semiquantitative analysis was measured by determining percentage of positive areas with ImageJ.

Immunofluorescence

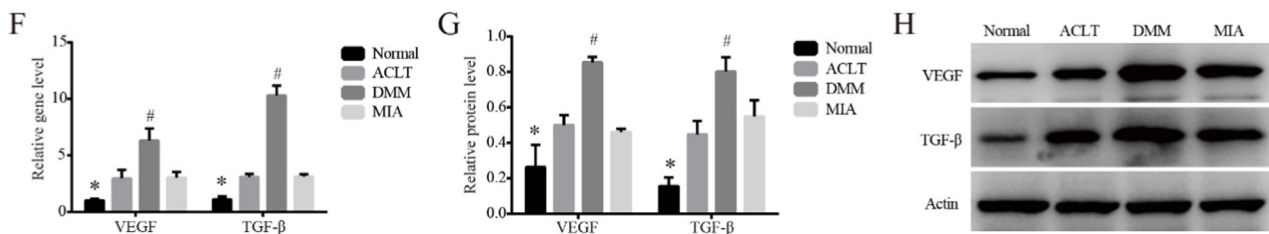
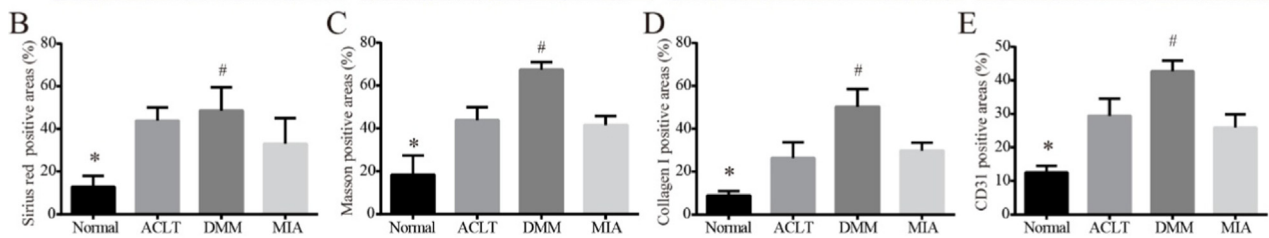
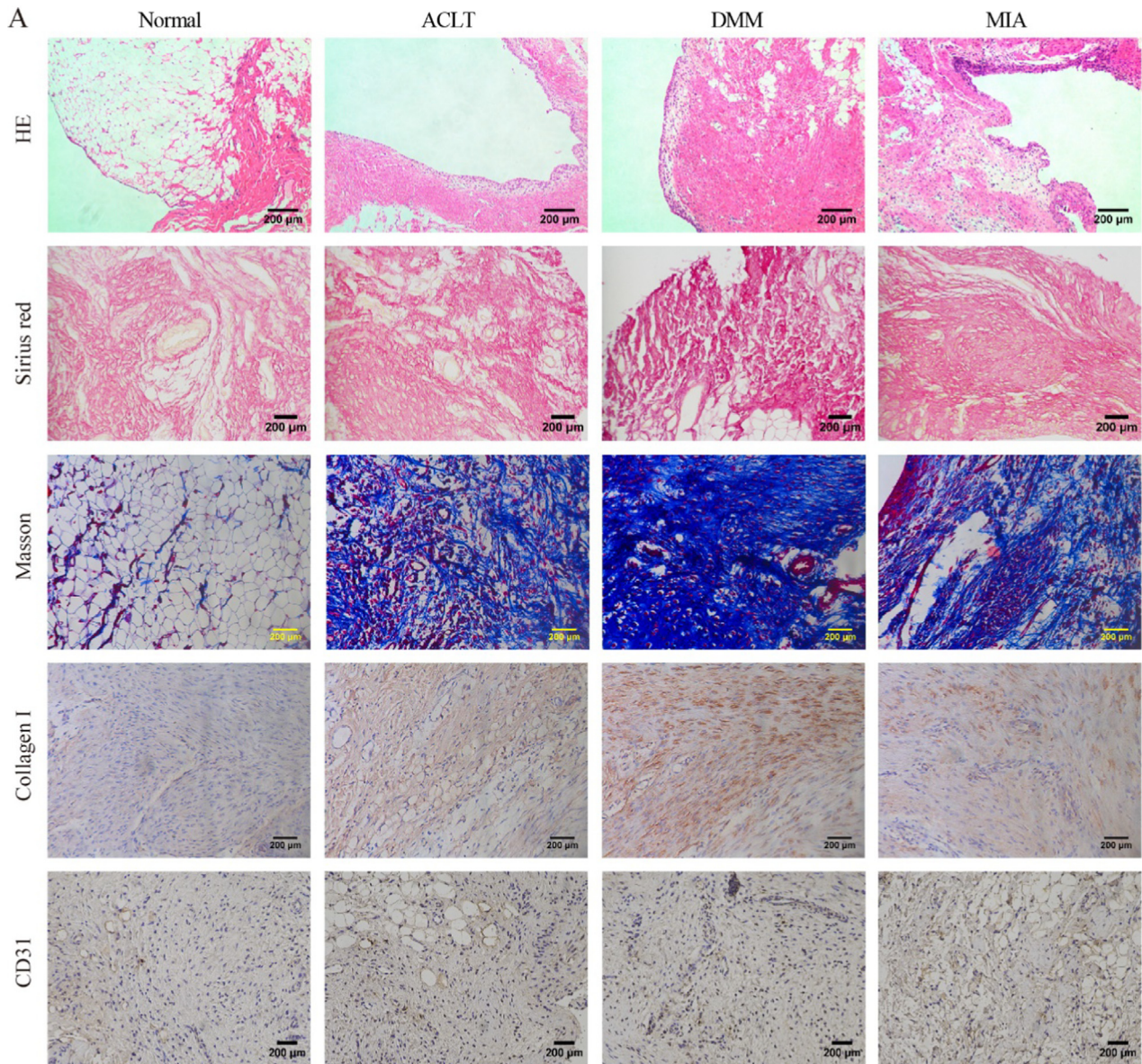
Briefly, antigen repair was carried out after the paraffin section was dehydrated, and autofluorescence quenching agent was added, then BSA. The primary antibody and the fluorescent secondary antibody were added successively. Attention was paid to the coloration of the species of the primary antibody and the color of the secondary antibody. Finally, the nucleus was stained by DAPI, and sections were observed and captured at the corresponding excitation wavelength using a Nikon Eclipse E100 (Nikon, Japan).

Quantitative real-time PCR

Total RNA was extracted with Trizol and assessed by spectrophotometer. Then, reverse transcription of RNA was performed using Prime Script RT reagent Kit (Beyotime Biotechnology, Shanghai, China). Primer was designed and synthesized by Shanghai Biotechnology Service Company in accordance with Gene sequence in GenBank Gene sequence design, together with Oligo v6.6 (Sequences as Table 1). qPCR was performed using Premix Ex Taq SYBR-Green PCR (Takara) according to the manufacturer's instructions on an ABI PRISM 7300 (Applied Biosystems, Foster City, CA, USA). The mRNA level of individual genes was normalized to GAPDH and calculated by the $2^{-\Delta\Delta CT}$ data analysis method.

Western blotting

Briefly, synovial or DRG tissues were mixed with RIPA lysate containing 0.1% PMSF and grinded for 10–15 min. Quantified the protein levels were with a BCA protein assay kit (Beyotime Biotechnology, Shanghai, China). Then samples were electrophoresed in SD-PAGE to separate protein bands, then transferred from gel onto PVDF membrane, blocked with 5% non-fat dry milk for 2 h. The membrane was incubated with first antibody (1:1000, Abcam, Cambridge, UK) for overnight at 4°C, and then second antibody (1:3000, Thermo Fisher Scientific, Shanghai, China) for 2 h. Later bands were visualized by exposure to ECL method and the overall gray value of protein bands was quantified, GAPDH as internal marker, namely, target protein gray value/ internal reference overall gray value.



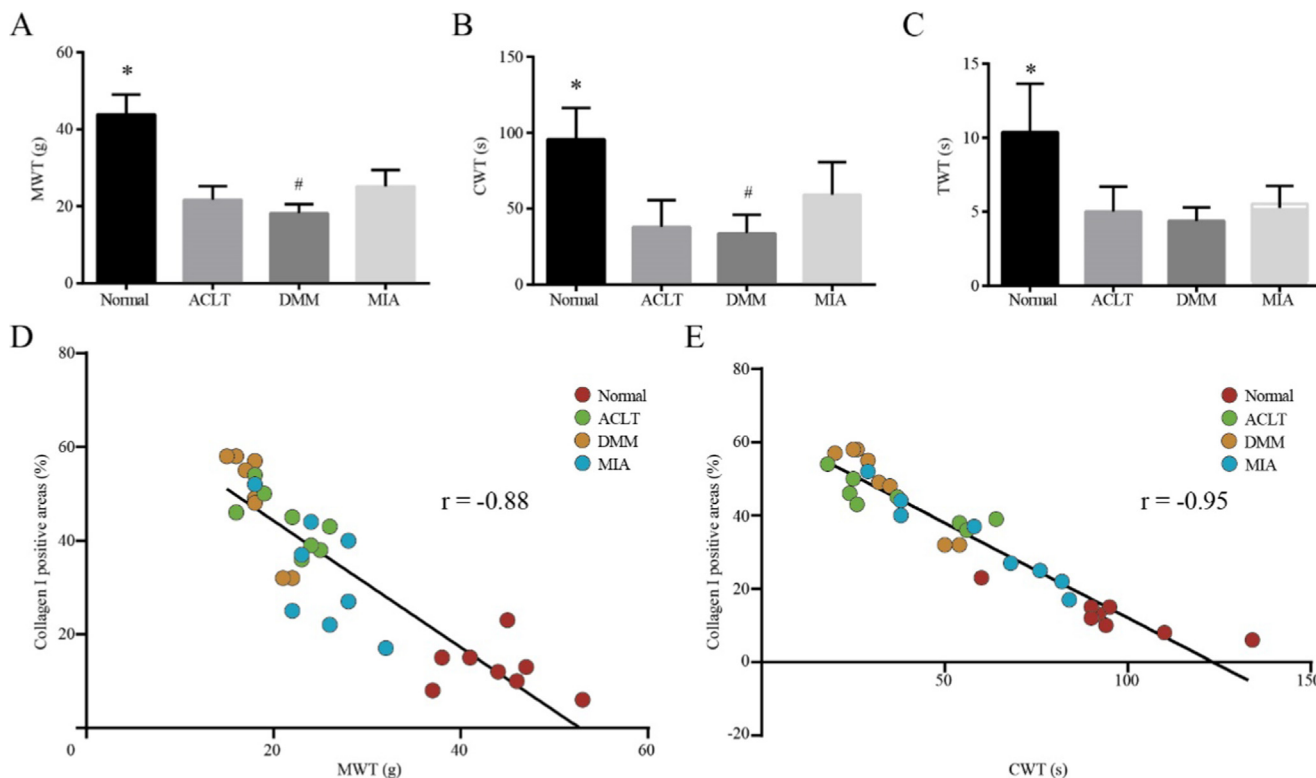


Fig. 2. Correlation between synovial fibrosis and pain behavior on Day14. (A). MWT value for rats in each group. * $P < 0.05$ vs. the other three groups, # $P < 0.05$ vs. the MIA. (B). CWT value for rats in each group. * $P < 0.05$ vs. the other three groups, # $P < 0.05$ vs. the MIA. (C). TWT value for rats in each group. * $P < 0.05$ vs. the other three groups. (D). Correlation analysis of synovial fibrosis degree and mechanical stimulation pain in rats. (E). Correlation analysis of synovial fibrosis degree and cold stimulation pain in rats.

Statistical analysis

All experiments were performed independently at least thrice, and data were presented as mean ± standard deviation (SD). Statistical analysis was performed using GraphPad Prism 6.0 Software (San Diego, CA, USA). Group comparisons were assessed with Student’s *t*-test or one-way ANOVA for comparison of multiple columns. A value of $P < 0.05$ (two-tailed) was considered as statistically significant. Pearson correlation tests were used to analyze the association between synovial fibrosis scores and data obtained from behavioral tests for KOA pain.

Results

Synovial fibrosis in KOA models on Day 14

We recorded the detailed process of modeling surgery (Supplemental Fig. 1A). In order to better show the anatomical results of the knee joint, the incision was enlarged appropriately, and the actual incision was much smaller. HE staining (Fig. 1A) showed increased inflammatory cell infiltration, disordered cell arrangement and augmented distance between nuclei, in the synovial lining layer of the three KOA model rats compared with that of the Normal group, which confirmed the successful establishment of the KOA model. In the Sirius Red stain, Masson stain and collage

I IHC for (Fig. 1A-D), synovial tissue of the three KOA models showed deeper collagen staining than that of the Normal, and the percentage of type I collagen positive area was increased ($P < 0.05$). Among them, the upregulation was the most obvious in DMM group, indicating synovial fibrosis was the most severe in the DMM group, which was statistically different from that in MIA group ($P < 0.05$). The IHC for CD31 showed the same trend (Fig. 1A, E). Consistent with this, both gene and protein expressions (Fig. 1F-H) of pro-fibrosis markers VEGF and TGF-β were higher in the three KOA models than in Normal ($P < 0.05$), and the level was the highest in the DMM group, which was statistically different from that in MIA ($P < 0.05$).

Correlation between synovial fibrosis and pain behavior on Day14

At Day 14, we measured the pain behavior of animals for the first time (Fig. 1A-C). The three groups of KOA model showed reduced tolerance to pain, and the values of MWT, CWT and TWT were all lower than that of Normal ($P < 0.05$). Besides, among the three groups of KOA models, rats in the DMM group were most sensitive to mechanical and cold stimuli, and the data of MWT and CWT were the lowest, which was statistically different than that of MIA ($P < 0.05$). However, no difference was observed between the three in TWT (Fig. 2C). In addition, we analyzed the correlation between the MWT and CWT values of the correspond-

Fig. 1. Synovial fibrosis in KOA models on Day 14. Notes: (A). Representative synovial tissues of each group stained with HE, 100×, scale bar = 200 μm. Sirius red and Masson stain for collagen I in synovial tissues of each group, 200×, scale bar = 200 μm. IHC for collagen I, CD31 in synovium of each group, 200×, scale bar = 200 μm. (B). Percentage of type I collagen positive area in Sirius red stain. * $P < 0.05$ vs. the other three groups, # $P < 0.05$ vs. the MIA. (C). Percentage of type I collagen positive area in Masson stain. * $P < 0.05$ vs. the other three groups, # $P < 0.05$ vs. the MIA. (D). Percentage of type I collagen positive area. * $P < 0.05$ vs. the other three groups, # $P < 0.05$ vs. the MIA. (E). Percentage of CD31 positive area. * $P < 0.05$ vs. the other three groups, # $P < 0.05$ vs. the MIA. (F). Relative gene expression of VEGF and TGF-β in synovial tissues. * $P < 0.05$ vs. the other three groups, # $P < 0.05$ vs. the MIA. (G). Relative protein level of VEGF and TGF-β in synovial tissues. * $P < 0.05$ vs. the other three groups, # $P < 0.05$ vs. the MIA. (H). Typical protein bands of VEGF and TGF-β.

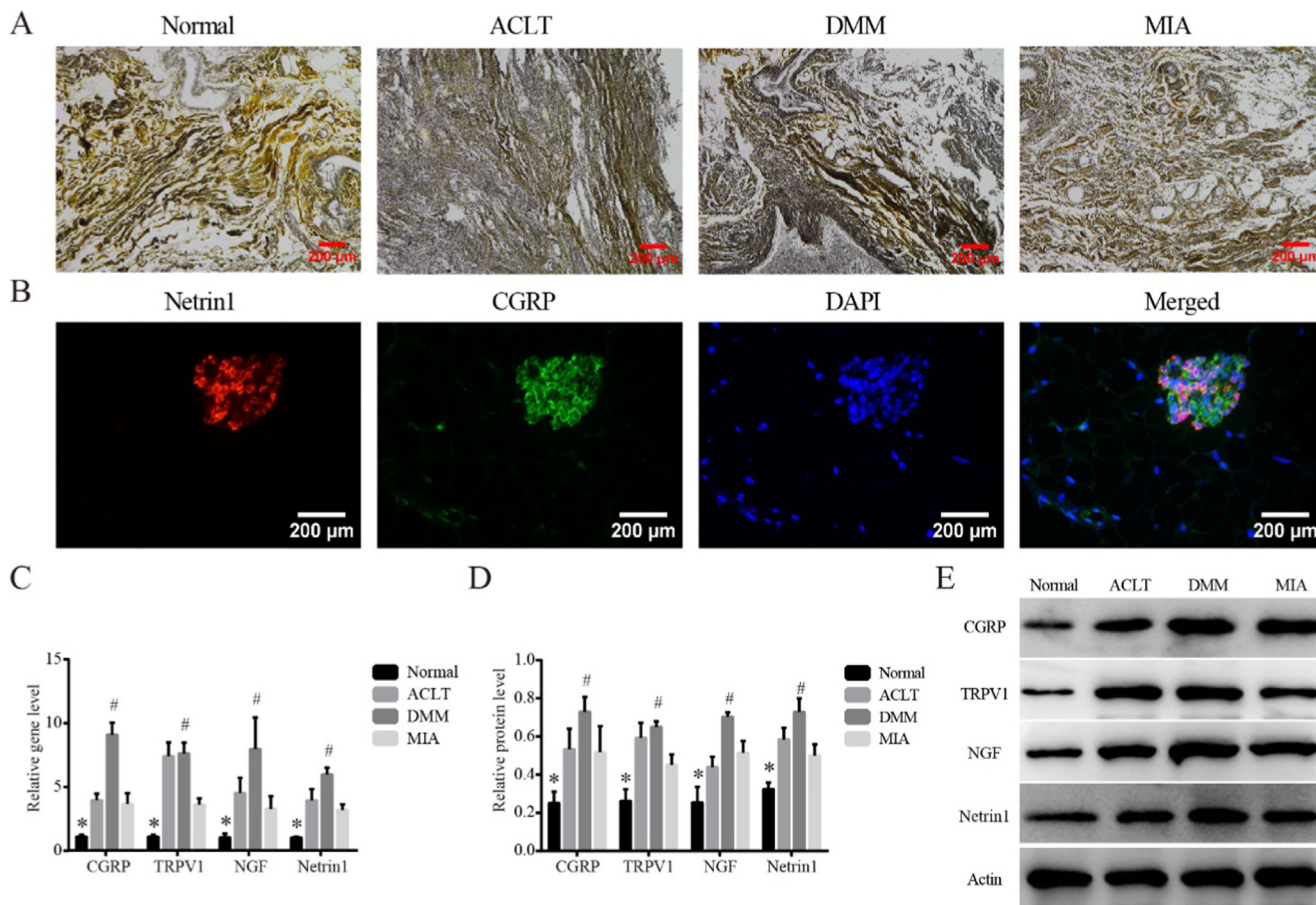


Fig. 3. Sensory innervation in synovium of rats within different KOA models on Day14. (A). Representative silver staining of synovial tissues in each group, 200×, scale bar = 200 μm. (B). Representative co-localization of Netrin1 and CGRP observed in synovium of DMM model, 400×, scale bar = 100 μm. (C). Relative gene expression of CGRP, TRPV1, NGF and Netrin1 in synovial tissues. **P* < 0.05 vs. the other three groups, #*P* < 0.05 vs. the MIA. (D). Relative protein level of CGRP, TRPV1, NGF and Netrin1 in synovial tissues. **P* < 0.05 vs. the other three groups, #*P* < 0.05 vs. the MIA. (E). Typical protein bands of CGRP, TRPV1, NGF and Netrin1.

ing numbered rats and the percentage of type I collagen (Fig. 2D, E), the R values were 0.88 and 0.95, respectively, which indicating that the degree of synovial fibrosis in rats with KOA was positively correlated with the sensitivity to mechanical stimulation pain and cold stimulation pain.

Sensory innervation in synovium of rats within different KOA models on Day14

To further investigate the sensory innervation in synovial tissue, silver staining which allowed the nerve fibers to appear black or brown was performed. Compared with Normal, synovium of the three KOA models showed deeper staining and wider positive area, suggesting increased sensory innervation (Fig. 3A). Subsequently, we examined the location of Netrin1 (Fig. 3B), an inducer of sensory innervation, in relation to CGRP positive nerves, as Netrin1 had been reported to play a key role in inducing increased sensory innervation in subchondral bone tissue. The co-localization of Netrin1 and CGRP was observed in all three groups of KOA models, suggesting that the increase in sensory innervation in synovium may also be related to Netrin1. In addition, we analyzed the expression of CGRP, TRPV1, NGF and Netrin1 which were closely related to pain sensation (Fig. 3C-E), consistent with the trend of pro-fibrosis markers, the above markers were upregulated in all KOA models than Normal (*P* < 0.05), and the difference was more significant in the DMM group than MIA (*P* < 0.05).

Changes in DRG tissue of different KOA models on Day14

To move one step further, we observed c-fos in DRG by immunofluorescence, as previous studies had confirmed the immediate early gene c-fos is rapidly and transiently expressed in neurons in response to stimulation. Consistent with that, the fluorescence intensity of c-fos in DRG of KOA animals in all three groups was higher than that in Normal (Fig. 4A). Besides, both mRNA and protein levels of CGRP, TRPV1, NGF and Netrin1 in DRG tissues were investigated (Fig. 4B-D). All the above markers were also upregulated in all KOA models than Normal (*P* < 0.05). Unexpectedly, only the expressions of CGRP and NGF were significantly increased in DMM compared with MIA (*P* < 0.05), while the expressions of TRPV1 and Netrin1 were not significantly different among the three groups.

Synovial fibrosis in KOA models on Day 28

At Day 28, we executed the remaining 10 rats in each group. Similar to Day 14, all the KOA models showed pathological features of synovitis and fibrosis (Fig. 5A). Interestingly, the synovial fibrosis in the ACLT model was the most typical among the three groups. The percentage of type I collagen positive area (Fig. 5B-D) was upregulated in ACLT compared with MIA (*P* < 0.05), while all the KOA models showed an increased positive percentage compared with Normal (*P* < 0.05). The IHC for CD31 showed the same

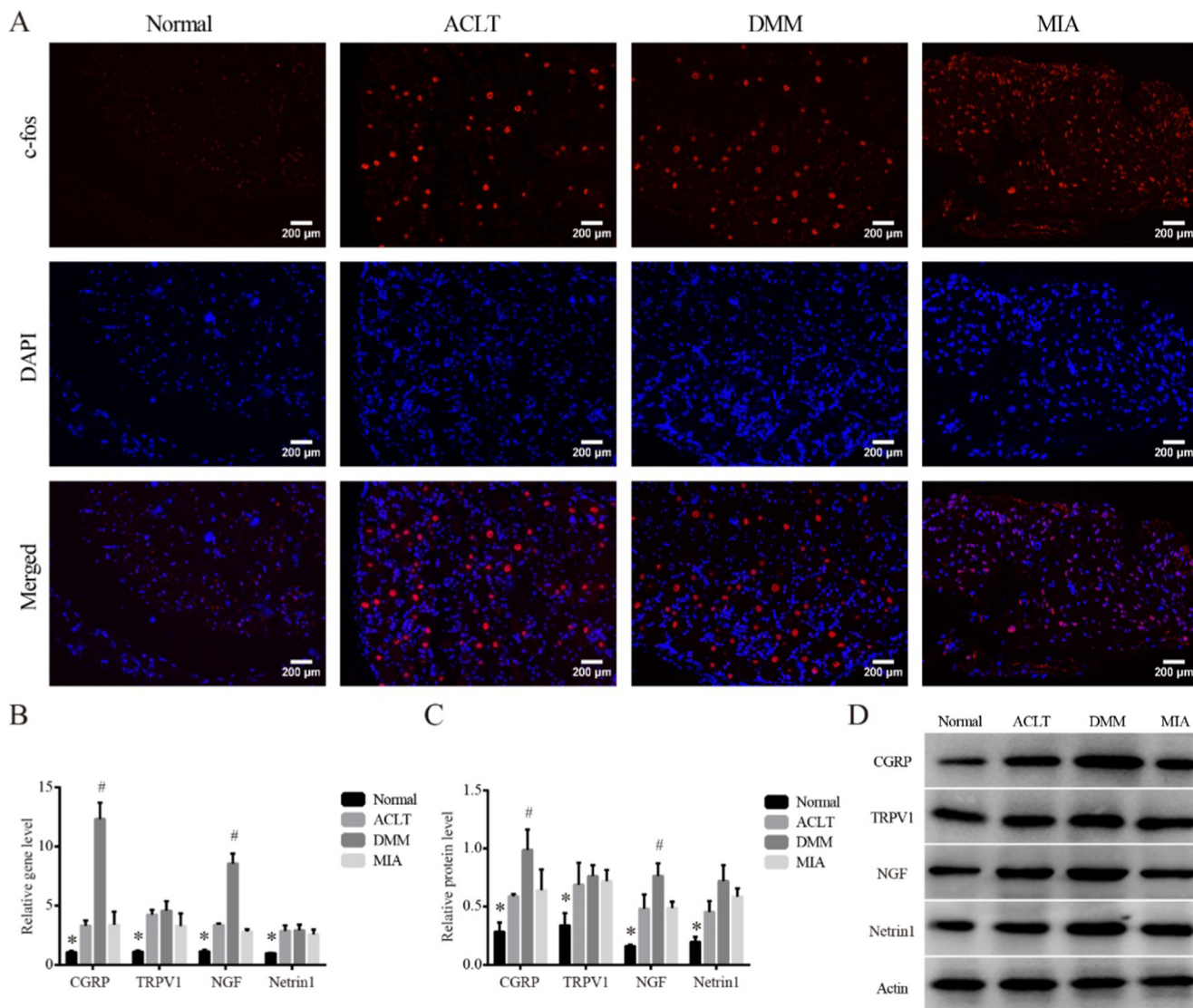


Fig. 4. Changes in DRG tissue of different KOA models on Day14. (A). Representative c-fos immunofluorescence for DRG tissues in each group, 200×, scale bar = 200 μm. (B). Relative gene expression of CGRP, TRPV1, NGF and Netrin1 in DRG tissues. **P* < 0.05 vs. the other three groups, #*P* < 0.05 vs. the MIA. (C). Relative protein level of CGRP, TRPV1, NGF and Netrin1 in DRG tissues. **P* < 0.05 vs. the other three groups, #*P* < 0.05 vs. the MIA. (D). Typical protein bands of CGRP, TRPV1, NGF and Netrin1.

trend (Fig. 1A, E). The gene and protein expressions of the fibrotic markers VEGF and TGF-β supported the characteristics observed by HE and Sirius red staining (Fig. 5F-H).

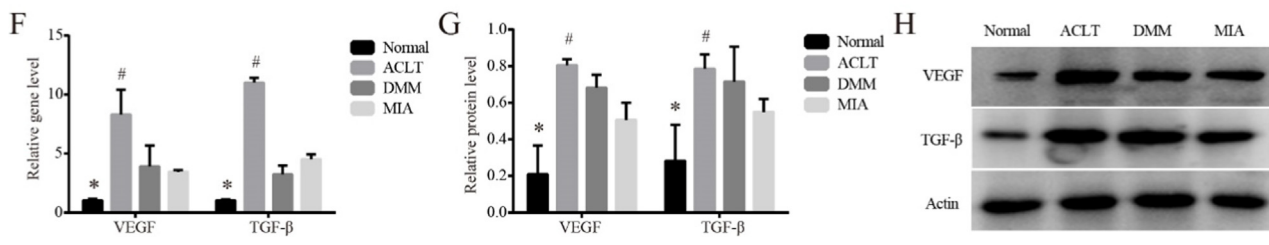
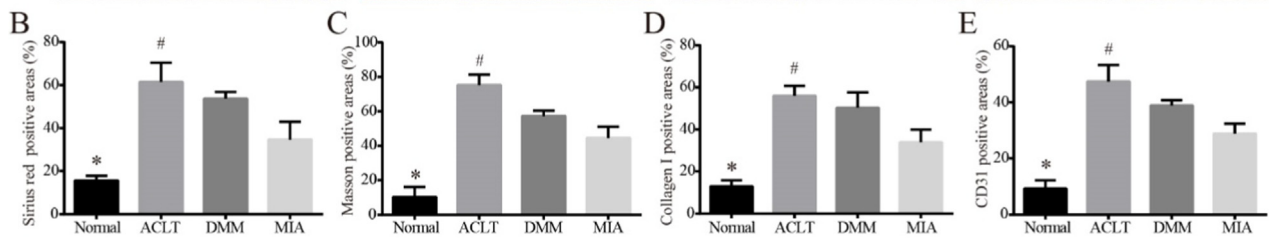
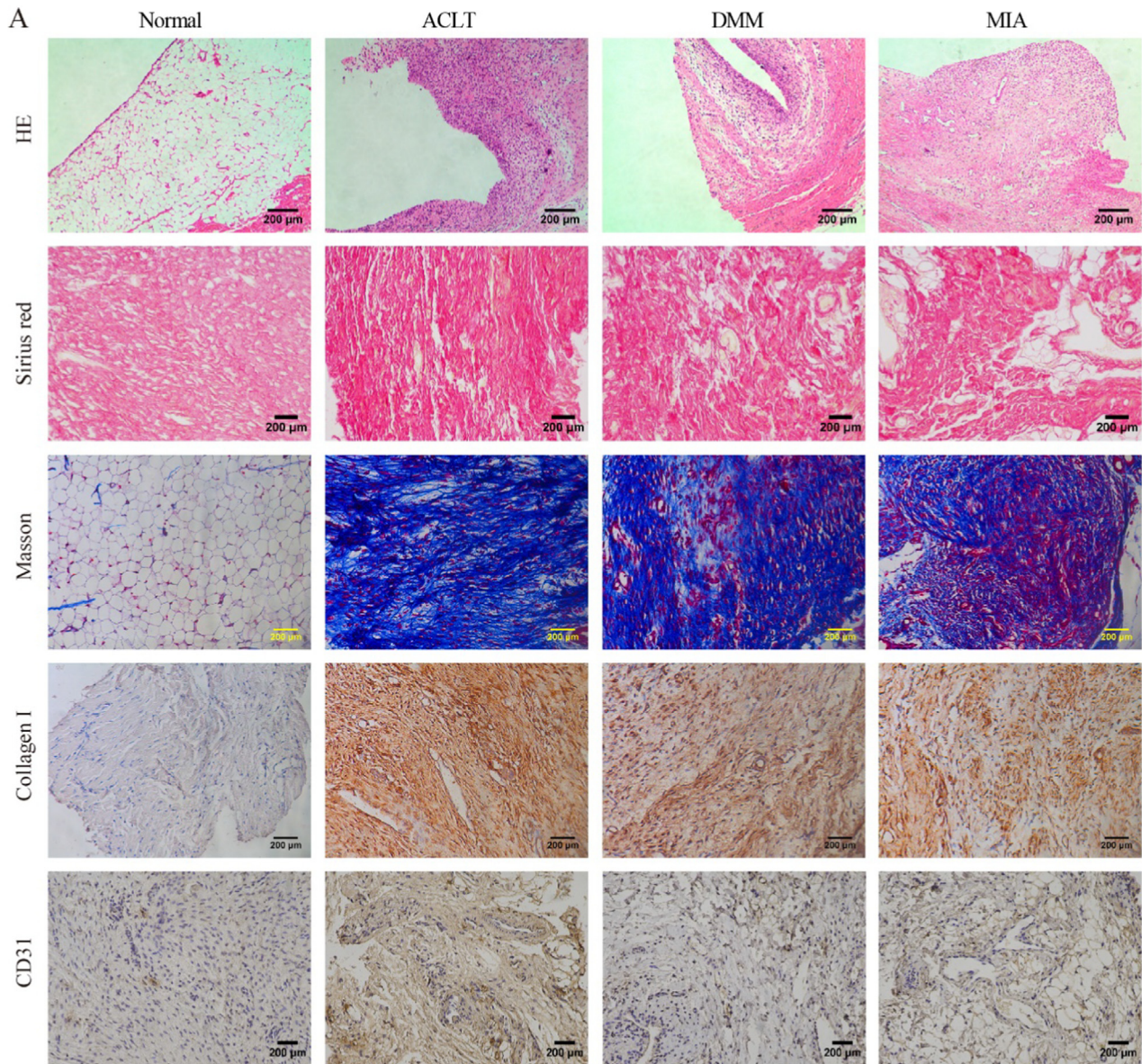
Sensory innervation associated changes within different KOA models on Day28

Finally, we observed the sensory innervation associated changes at 28 days in the synovial tissue and DRG tissue within different KOA models, respectively. As shown in Fig. 6A, silver staining of synovial tissue in the three KOA models showed more neuronal axon staining than normal, which was consistent with the degree of synovial fibrosis, and ACLT seemed to be the most prominent group. Besides, both mRNA and protein level (Fig. 6B-D) of CGRP, TRPV1, NGF and Netrin1 in were also upregulated in all KOA models compared with Normal (*P* < 0.05). Meanwhile, the expressions of all the above markers were significantly increased in ACLT compared with MIA (*P* < 0.05), but were not always significantly different between ACLT and DMM. In addition, higher fluorescence intensity of c-fos (Supplemental Fig. 2A) were observed in DRG of all the KOA model rats, indicating the continu-

ous existence of injury stimulus signals. Interestingly, although the protein expression of CGRP, TRPV1, NGF and Netrin1 in DRG was higher in KOA model groups than that in Normal, there was no difference among the three KOA models (Supplemental Fig. 2B, C).

Discussion

In this study, we constructed three commonly used KOA models, including two surgical models and one chemical drug injection model. HE staining of synovium were used to confirm the establishment of the KOA model. On the 14th and 28th day after modeling, all the KOA synovium showed higher percentage of type I collagen, increased expression of CD31, VEGF and TGF-β, indicating a greater degree of synovial fibrosis. These findings were consistent with the others, who reported elevated VEGF and TGF-β in ACLT, DMM, or MIA models, not only in the synovium, but even in subchondral bone or the synovial fluid [26–29]. Meanwhile, the central role of TGF and VEGF in fibrosis cascade had been widely recognized. Notably, the two types of surgically induced KOA model showed more serious synovial fibrosis than the MIA model



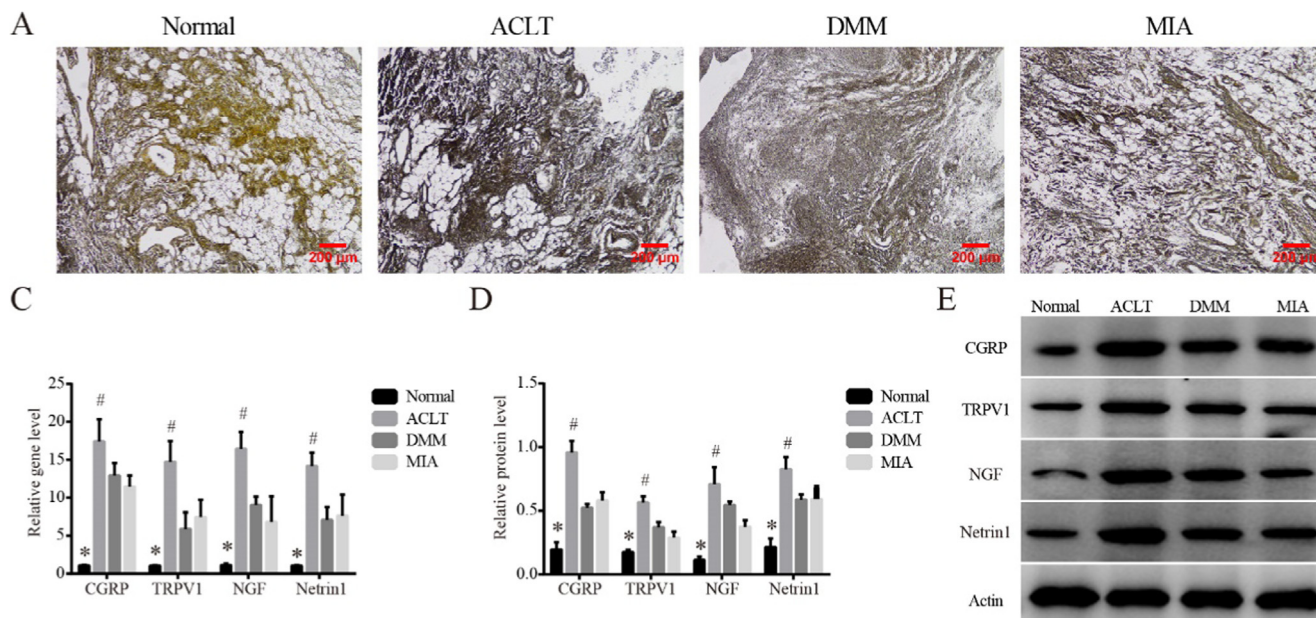


Fig. 6. Sensory innervation associated changes within different KOA models on Day 28. (A). Representative silver staining of synovial tissues in each group, 200 \times , scale bar = 200 μ m. (B). Relative gene expression of CGRP, TRPV1, NGF and Netrin1 in synovial tissues. * $P < 0.05$ vs. the other three groups, # $P < 0.05$ vs. the MIA. (C). Relative protein level of CGRP, TRPV1, NGF and Netrin1 in synovial tissues. * $P < 0.05$ vs. the other three groups, # $P < 0.05$ vs. the MIA. (D). Typical protein bands of CGRP, TRPV1, NGF and Netrin1.

at both Day 14 and Day 28, with DMM presenting the most prominent synovial fibrosis at day 14 and ACLT at day 28. We could not neglect the effect of surgical modeling itself on synovial fibrosis, but in practice, ACLT often had the largest surgical wound. Therefore, in the process of synovial fibrosis formation in KOA model, the DMM model might be more intense in the short term than the ACLT model, while the influence of ACLT would last longer. Besides, the fibrosis process generated by MIA model excludes the influence of surgery, and it may better simulate the synovial fibrosis process of human KOA. Similarly, Glasson SS et al. evaluated the ACLT and DMM at 4 weeks, 8 weeks post-surgery and confirmed the ACLT model gave severe OA, while DMM was less invasive than the ACLT procedure [24]. It was also reported that ACLT had more significant pain from the first week after surgery than the KOA model induced with surgically cartilage injury [30].

On the other hand, we compared the pain behavior of rats in each group on Day 14. Compared with the Normal group, all the three KOA models showed obvious sensitivity to mechanical, cold and thermal stimulation. No difference was observed in thermal hyperalgesia among the three models, while changes in mechanical hyperalgesia and cold thermal hyperalgesia were similar to the degree of synovial fibrosis, which were most typical in DMM model and statistically different from MIA model. Therefore, we analyzed the correlation between the MWT and CWT values of the corresponding numbered rats and the percentage of type I collagen. There was a negative correlation between the percentage of type I collagen and MWT ($r = -0.88$), suggesting that the more severe the synovial fibrosis, the more sensitive the mechanical hyperalgesia. The same trend also occurred between the percentage of

type I collagen and CWT ($r = -0.95$). In concordance with current observations, inflammatory cell infiltration to the infrapatellar fat pad was observed on day 3 and reached synovial membrane on day 7 after MIA injection, according to Inomata K et al., and they also proved that the extensive fibrosis throughout the infrapatellar fat pad plays critical roles during persistent pain development in KOA [31]. Besides, in clinical trials, the degree of synovial thickening on magnetic resonance imaging was correlated with qualitative microscopic features such as surface fibrin deposition, fibrosis [32]. And these thickening of the synovial membrane was the result of an overexpression of type III collagen shifting the turnover balance towards formation instead of degradation, linked to KOA pain sensitization [33]. We did not repeat this experiment at Day 28 because the MIA-induced KOA model, although time-dose-dependent, still showed faster progression of KOA than the surgical model [34]. Besides, due to the possible neurotoxicity caused by MIA, KOA structural pathology as measured only partially explains the MIA-induced phenotype [15,35]. In addition, it had also been reported that synovitis and pain sensitivity induced by MIA presented some self-healing characteristics, even within 14 days [36–38].

Subsequently, sensory innervation changes associated with pain sensitization in synovial and DRG tissues were observed. On Day 14, silver staining revealed more axonal staining in the synovial tissue of DMM model than other model groups, indicating the increase of nerve fiber density. The gene and protein expressions of CGRP and TRPV1 in each model group were higher than those in the normal group, and the highest was found in the DMM group, which had a statistical difference compared with

Fig. 5. Synovial fibrosis in KOA models on Day 28. (A). Representative synovial tissues of each group stained with HE, 100 \times , scale bar = 200 μ m. Sirius red and Masson stain for collagen I in synovial tissues of each group, 200 \times , scale bar = 200 μ m. IHC for collagen I, CD31 in synovium of each group, 200 \times , scale bar = 200 μ m. (B). Percentage of type I collagen positive area in Sirius red stain. * $P < 0.05$ vs. the other three groups, # $P < 0.05$ vs. the MIA. (C). Percentage of type I collagen positive area in Masson stain. * $P < 0.05$ vs. the other three groups, # $P < 0.05$ vs. the MIA. (D). Percentage of type I collagen positive area. * $P < 0.05$ vs. the other three groups, # $P < 0.05$ vs. the MIA. (E). Percentage of CD31 positive area. * $P < 0.05$ vs. the other three groups, # $P < 0.05$ vs. the MIA. (F). Relative gene expression of VEGF and TGF- β in synovial tissues. * $P < 0.05$ vs. the other three groups, # $P < 0.05$ vs. the MIA. (G). Relative protein level of VEGF and TGF- β in synovial tissues. * $P < 0.05$ vs. the other three groups, # $P < 0.05$ vs. the MIA. (H). Typical protein bands of VEGF and TGF- β .

MIA, but no statistical difference compared with ACLT, suggesting that the increase of CGRP-labeled nerve fibers and nociceptor TRPV1 was most significant in the synovial tissue of the DMM model. Pain mediator NGF and Netrin1 showed the same trend. The subsequent immunofluorescence co-localization of Netrin1 and CGRP confirmed that the location of the two in synovial tissue was highly consistent, suggesting that the guiding effect of axonal guidance factors on CGRP-labeled neurons might be the potential cause of increased sensory innervation. Notably, the difference of Netrin1 expression within KOA models were only observed in synovial tissue, but not in DRG, indicating that Netrin1 is more likely to be produced through local tissue cells of knee joint. Although the origin of Netrin1 could not be determined, it could be speculated that the increased sensory innervation might be highly correlated with Netrin1. Consistently, as an axon guidance, Netrin1 signals were not only required in axon outgrowth and disassembly of adhesive structures together with cytoskeletal dynamics, but also necessary in regulating patterning of the vascular system, involved in the pathological process of KOA, especially peripheral sensitization [14,39,40]. At Day 28, the changes observed in synovial tissues in each group were roughly the same as those observed at Day 14. Notably, ACLT replaced DMM as the most representative KOA model, both in terms of the degree of synovial fibrosis and the levels of indicators related to sensory nerve innervation including CGRP, TRPV1, NGF and Netrin1.

Meanwhile, in DRG tissue, c-fos showed higher fluorescence intensity in each model group than the Normal at both Day 14 and 28, suggesting that in KOA model, DRG continuously responded to harmful stimuli. The expression levels of CGRP, TRPV1, NGF and Netrin1 in all model groups were higher than those in Normal, suggesting that DRG was involved in the peripheral sensitization and sensory nerve innervation of KOA. Interestingly, only at Day 14, the levels of CGRP and NGF were observed to be different among the three model groups, and the highest in the DMM model group, which was statistically different than that in the MIA group. At Day 28, these indicators did not differ between the three model groups, and it seemed that once KOA peripheral sensitization was established, DRG would respond to stimulation in an independent manner, rather than depending on the signals from the knee. But such a view requires further observation.

In previous studies, it seems that all the methods used to construct KOA have been used to study KOA pain, because they all mimic the local pathological changes in KOA and induce pain sensation [13]. However, in this study, we observed that from 14 days after modeling, synovial fibrosis and sensory innervation of ACLT increased more rapidly than that of DMM and MIA, showing more advantages in pain research. The gentler development of DMM may be more suitable for smaller animals, such as mice [14], and MIA cannot simulate the pathological changes of human KOA as well as ACLT. Combined with other studies supporting ACLT, we believe that ACLT is more applicable for KOA pain research.

In summary, we found evidence of increased sensory innervation in three animal models commonly used for KOA, and the degree of synovial fibrosis was positively correlated with pain sensitivity to KOA mechanical stimulation and cold mechanical stimulation. We found that surgical modeling was more suitable for the study of KOA pain and pain sensitivity. The DMM model had higher degree of fibrosis, more obvious pain sensitivity, and more intensive sensory innervation at 14 days of modeling, while the ACLT model had more advantages at 28 days and longer. Combined with the observation and comparison of the above models used to simulate KOA in previous studies [14,30,34], ACLT is more recommended in the selection of KOA models in the future. However, the current study still has a few limitations. Although we observed relationships between structural histopathology and pain, we can-

not fully conclude that the pain observed in these rats are primarily mediated by the pathology. The increased sensory innervation is only one possibility of the relationship observed between KOA synovial fibrosis and pain sensitivity.

Conclusions

In conclusion, this study confirmed that there is an increase in pain-related sensory innervation in synovial and DRG tissues of KOA rat model, which may be the structural basis of peripheral pain sensitivity of KOA. Besides, the degree of synovial fibrosis was positively correlated with pain sensitivity to KOA mechanical stimulation and cold mechanical stimulation in model rats. Additionally, surgical modeling appears to be more advantageous in the field of pain research in KOA than MIA, not only because of the more sensitive pain behavioral characteristics, but also the more abundant sensory innervation. ACLT method is more recommended for KOA pain research in the future.

Data availability statements

The data used to support the findings of this study are available from the corresponding author upon request.

Compliance with ethics requirements

All Institutional and National Guidelines for the care and use of animals (fisheries) were followed.

CRediT authorship contribution statement

Li Zhang: Data curation, Writing - original draft, Validation. **Mingchao Li:** Investigation. **Xiaochen Li:** Investigation. **Taiyang Liao:** Investigation, Resources, Software. **Zhenyuan Ma:** Investigation, Resources. **Li Zhang:** Formal analysis, Software. **Runlin Xing:** Formal analysis. **Peimin Wang:** Conceptualization, Methodology, Supervision, Funding acquisition. **Jun Mao:** Project administration, Data curation, Writing - review & editing, Funding acquisition.

Declaration of Competing Interest

The authors declare that they have no known competing financial interests or personal relationships that could have appeared to influence the work reported in this paper.

Acknowledgments

The current work was supported by the National Natural Science Foundation of China (No.82074460, No.81774334); the Leading Talents of Traditional Chinese Medicine Project (k2018j07); Jiangsu Province Postgraduate Training Innovation Project (KYCX20_1463). The authors would like to thank the Key Laboratory for Metabolic Diseases in Chinese Medicine, Nanjing University of Chinese Medicine, for their help.

Appendix A. Supplementary material

Supplementary data to this article can be found online at <https://doi.org/10.1016/j.jare.2021.06.007>.

References

- [1] Conaghan PG, Cook AD, Hamilton JA, et al. Therapeutic options for targeting inflammatory osteoarthritis pain. *Nat Rev Rheumatol* 2019;15(6):355–63.
- [2] Hunter DJ, Bierma-Zeinstra S. Osteoarthritis. *Lancet* 2019;393(10182):1745–59.

- [3] Sharma L. Osteoarthritis of the Knee. *N Engl J Med* 2021;384(1):51–9.
- [4] Rim YA, Ju JH. The Role of Fibrosis in Osteoarthritis Progression. *Life (Basel)* 2020;11(1):3.
- [5] Remst DF, Blaney Davidson EN, van der Kraan PM. Unravelling osteoarthritis-related synovial fibrosis: a step closer to solving joint stiffness. *Rheumatology (Oxford)* 2015;54(11):1954–63.
- [6] Harris JA. Using c-fos as a neural marker of pain. *Brain Res Bull* 1998;45(1):1–8.
- [7] da Silva MR, Linhares D, Vasconcelos DM, et al. Neuroimmune expression in hip osteoarthritis: a systematic review. *BMC Musculoskelet Disord* 2017;18(1):394.
- [8] Mlost J, Kostrzewa M, Malek N, Starowicz K. Molecular Understanding of the Activation of CB1 and Blockade of TRPV1 Receptors: Implications for Novel Treatment Strategies in Osteoarthritis. *Int J Mol Sci* 2018;19(2):342.
- [9] Montagnoli C, Tiribuzi R, Crispoltoni L, et al. β -NGF and β -NGF receptor upregulation in blood and synovial fluid in osteoarthritis. *Biol Chem* 2017;398(9):1045–54.
- [10] Dai S, Liang T, Fujii T, et al. Increased elastic modulus of the synovial membrane in a rat ACLT model of osteoarthritis revealed by atomic force microscopy. *Braz J Med Biol Res* 2020;53(11):e10058.
- [11] Yang Y, Li P, Zhu S, et al. Comparison of early-stage changes of osteoarthritis in cartilage and subchondral bone between two different rat models. *PeerJ* 2020;20(8):e8934.
- [12] Barbosa GM, Cunha JE, Russo TL, et al. Thirty days after anterior cruciate ligament transection is sufficient to induce signs of knee osteoarthritis in rats: pain, functional impairment, and synovial inflammation. *Inflamm Res* 2020;69(3):279–88.
- [13] Miller RE, Malfait AM. Osteoarthritis pain: What are we learning from animal models?. *Best Pract Res Clin Rheumatol* 2017;31(5):676–87.
- [14] Glasson SS, Blanchet TJ, Morris EA. The surgical destabilization of the medial meniscus (DMM) model of osteoarthritis in the 129/SvEv mouse. *Osteoarthritis Cartilage* 2007;15(9):1061–9.
- [15] Obeidat AM, Miller RE, Miller RJ, Malfait AM. The nociceptive innervation of the normal and osteoarthritic mouse knee. *Osteoarthritis Cartilage* 2019;27(11):1669–79.
- [16] Zhu S, Zhu J, Zhen G, et al. Subchondral bone osteoclasts induce sensory innervation and osteoarthritis pain. *J Clin Invest* 2019;129(3):1076–93.
- [17] Murakami K, Nakagawa H, Nishimura K, et al. Changes in peptidergic fiber density in the synovium of mice with collagenase-induced acute arthritis. *Can J Physiol Pharmacol* 2015;93(6):435–41.
- [18] Aso K, Izumi M, Sugimura N, et al. Nociceptive phenotype alterations of dorsal root ganglia neurons innervating the subchondral bone in osteoarthritic rat knee joints. *Osteoarthritis Cartilage* 2016;24(9):1596–603.
- [19] Pujol R, Girard CA, Richard H, Hassanpour I, Binette MP, Beauchamp G, et al. Synovial nerve fiber density decreases with naturally-occurring osteoarthritis in horses. *Osteoarthritis Cartilage* 2018;26(10):1379–88.
- [20] van der Kraan PM. The changing role of TGF β in healthy, ageing and osteoarthritic joints. *Nat Rev Rheumatol* 2017;13(3):155–63.
- [21] MacDonald IJ, Liu SC, Su CM, et al. Implications of Angiogenesis Involvement in Arthritis. *Int J Mol Sci* 2018;19(7):2012.
- [22] Chen Y, Qiu F, Zhu X, et al. Pannus does not occur only in rheumatoid arthritis: a pathological observation of pannus of knee osteoarthritis. *Nan Fang Yi Ke Da Xue Xue Bao* 2019;39(6):747–50.
- [23] Ashraf S, Mapp PI, Walsh DA. Contributions of angiogenesis to inflammation, joint damage, and pain in a rat model of osteoarthritis. *Arthritis Rheum* 2011;63(9):2700–10.
- [24] Takano S, Uchida K, Itakura M, et al. Transforming growth factor- β stimulates nerve growth factor production in osteoarthritic synovium. *BMC Musculoskelet Disord* 2019;20(1):204.
- [25] Lee SY, Lee SH, Na HS, et al. The Therapeutic Effect of STAT3 Signaling-Suppressed MSC on Pain and Articular Cartilage Damage in a Rat Model of Monosodium Iodoacetate-Induced Osteoarthritis. *Front Immunol* 2018;11(9):2881.
- [26] Luo Q, Fan S, Li R, et al. Effects of ultrasound on vascular endothelial growth factor in cartilage, synovial fluid, and synovium in rabbit knee osteoarthritis. *Acta Biochim Pol* 2020;67(3):379–85.
- [27] Mu W, Xu B, Ma H, et al. Halofuginone attenuates articular cartilage degeneration by inhibition of elevated TGF- β 1 signaling in articular cartilage in a rodent osteoarthritis model. *Mol Med Rep* 2017;16(5):7679–84.
- [28] Wang PE, Zhang L, Ying J, et al. Bushenhuoxue formula attenuates cartilage degeneration in an osteoarthritic mouse model through TGF- β /MMP13 signaling. *J Transl Med* 2018;16(1):72.
- [29] Yamairi F, Utsumi H, Ono Y, et al. Expression of vascular endothelial growth factor (VEGF) associated with histopathological changes in rodent models of osteoarthritis. *J Toxicol Pathol* 2011;24(2):137–42.
- [30] Tawonsawatruk T, Sriwatananukulkit O, Himakhun W, et al. Comparison of pain behaviour and osteoarthritis progression between anterior cruciate ligament transection and osteochondral injury in rat models. *Bone Joint Res* 2018;7(3):244–51.
- [31] Inomata K, Tsuji K, Onuma H, et al. Time course analyses of structural changes in the infrapatellar fat pad and synovial membrane during inflammation-induced persistent pain development in rat knee joint. *BMC Musculoskelet Disord* 2019;20(1):8.
- [32] Loeuille D, Chary-Valckenaere I, Champigneulle J, et al. Macroscopic and microscopic features of synovial membrane inflammation in the osteoarthritic knee: correlating magnetic resonance imaging findings with disease severity. *Arthritis Rheum* 2005;52(11):3492–501.
- [33] Petersen KK, Siebuhr AS, Graven-Nielsen T, et al. Sensitization and Serological Biomarkers in Knee Osteoarthritis Patients With Different Degrees of Synovitis. *Clin J Pain* 2016;32(10):841–8.
- [34] Gervais JA, Otis C, Lussier B, et al. Osteoarthritic pain model influences functional outcomes and spinal neuropeptidomics: A pilot study in female rats. *Can J Vet Res* 2019;83(2):133–41.
- [35] Otis C, Gervais J, Guillot M, et al. Concurrent validity of different functional and neuroproteomic pain assessment methods in the rat osteoarthritis monosodium iodoacetate (MIA) model. *Arthritis Res Ther* 2016;23(18):150.
- [36] de Sousa Valente J. The Pharmacology of Pain Associated With the Monoiodoacetate Model of Osteoarthritis. *Front Pharmacol* 2019;18(10):974.
- [37] Xu J, Yan L, Yan B, et al. Osteoarthritis Pain Model Induced by Intra-Articular Injection of Mono-Iodoacetate in Rats. *J Vis Exp* 2020(159).
- [38] Yamada EF, Salgueiro AF, Goulart ADS, et al. Evaluation of monosodium iodoacetate dosage to induce knee osteoarthritis: Relation with oxidative stress and pain. *Int J Rheum Dis* 2019;22(3):399–410.
- [39] Sato T, Kokabu S, Enoki Y, et al. Functional Roles of Netrin-1 in Osteoblast Differentiation. *Vivo* 2017;31(3):321–8.
- [40] Sheng J, Liu D, Kang X, et al. Egr-1 increases angiogenesis in cartilage via binding Netrin-1 receptor DCC promoter. *J Orthop Surg Res* 2018;13(1):125.